Sensors and Actuators B 199 (2014) 339–345

Contents lists available at ScienceDirect

Sensors and Actuators B: Chemical

journal homepage: www.elsevier.com/locate/snb

High-performance gas sensor based on ZnO nanowires functionalized by Au nanoparticles

Jing Guo, Jun Zhang*, Min Zhu, Dianxing Ju, Hongyan Xu, Bingqiang Cao*

Key Laboratory of Inorganic Functional Materials in Universities of Shandong, School of Materials Science and Engineering, University of Jinan, West Road of NanXinZhuang 336, Jinan 250022, China

ARTICLE INFO

Article history:
Received 12 December 2013
Received in revised form 21 January 2014
Accepted 3 April 2014
Available online 16 April 2014

Keywords:
ZnO
Nanorods
Au
Sensor
High performance

ABSTRACT

One-dimensional (1D) semiconductor nanostructure has been widely used for gas sensor devices. In this work, a high performance gas sensor based on Au-functionalized ZnO nanorods was fabricated. Au nanoparticles were successfully immobilized onto the surface of ZnO nanorods to serve as a sensitizer by a facile solution reduction process. The hybrid Au/ZnO nanorods have been systematically characterized by XRD, SEM, EDS, TEM and optical absorption spectrum. Gas sensing tests reveal that the Au/ZnO sensor has remarkably enhanced performance compared to pure ZnO. It could detect ethanol gas in a wide concentration range with very high response, fast response–recovery time, good selectivity and stable repeatability. The possible sensing mechanism is discussed. The superior sensing features indicate the present Au/ZnO nanorods are promising for gas sensors.

1. Introduction

One-dimensional (1D) oxide semiconductor nanostructures, such as nanowires, nanorods, nanotubes, nanofibers and nanobelts, have been widely used for various applications, like gas sensors [1–3], solar cells [4], lithium ion batteries [5] and other optoelectronic nanodevices [6–9], which benefit from the advantageous high surface-to-volume ratio and high electron mobility along the growth direction of 1D nanostructure. Furthermore, the good chemical and thermal stability of 1D nanostructure could ensure stable device performance, because the 1D structure is not easily sintered at a relatively high temperature. In particular, when used for gas sensor, the 1D nanostructure has proven to exhibit good performances [2,10–12]. In order to satisfy the increasing demand in gas sensors for high quality application, it is of great importance to further improve the sensor performance to acquire lower detection limit, higher response, faster response and recovery time and better selectivity. Moreover, practical applications also require a sensor that is able to detect target gases over a wide concentration range.

SnO_2, ZnO and Fe_2O_3 nanomaterials have been widely investigated for gas sensor due to their nontoxicity, stability and low cost. Though they manifest good performance, some problems still exist. Mandayo et al. [13] have reported that SnO_2 thin film tends to stabilize after approximate 25 days, but the selectivity to target carbon monoxide seems to decrease during the test. Ramgir et al. [14] have shown that the response of ZnO modified with Au nanoparticles exhibits small fluctuation to 50 ppm ethanol in less than two weeks. The response of different α-Fe_2O_3 nanoparticles synthesized by Cao's group [15] shows decrease after 30 days. The common problems they encounter are low response and poor stability that cannot ensure a long sensor life [1,13–15]. Furthermore, chemresistive gas sensors based on metal oxide semiconductors usually suffer from a narrow detection range of target gas concentration, because they show severe saturation when the gas concentration is over 300 ppm [16–18]. For example, the sensor response of α-Fe_2O_3 urchin-like spheres synthesized by Sun [18] only shows a linear increase to ethanol concentration less than 200 ppm. This will restrict their application in high gas concentration environment. A promising solution to these problems is to functionalize metal oxides with catalytic metal nanoparticles [3,19–21]. As we all know, Au is a typical noble metal with some superior properties, which could promote the gas sensor performance of various ZnO nanostructures including nanorods [22,23], nanowire [24,25], hollow spheres [26] and nanoflowers [27]. However, these gas sensors failed to exhibit a satisfactory response to gas concentration over 500 ppm.

In this contribution, a high-performance gas sensor was fabricated using Au sensitized ZnO nanorods. ZnO nanorods prepared by hydrothermal method were functionalized with Au nanoparticles

* Corresponding authors. Tel.: +86 531 8973 6292; fax: +86 531 8276 4453.
E-mail addresses: mse_zhangj@ujn.edu.cn (J. Zhang), mse_caobq@ujn.edu.cn (B. Cao).

http://dx.doi.org/10.1016/j.snb.2014.04.010
0925-4005/

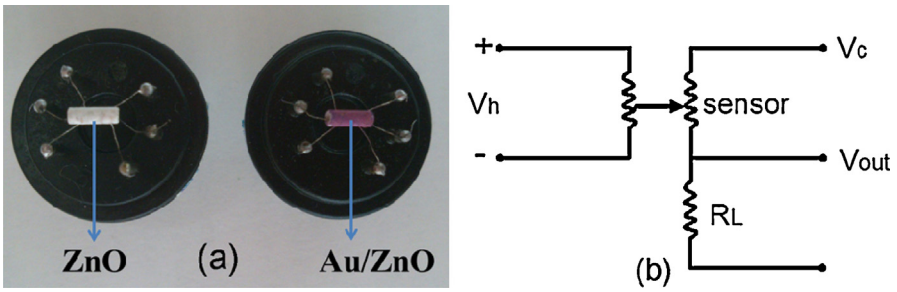

Fig. 1. (a) Optical image of gas sensors based on ZnO and Au/ZnO nanorods, (b) working principle of gas sensing measurement, V_h, V_c, V_{out}, and R_L are heating voltage, circuit voltage, output voltage, and loading resistance, respectively.

by a solution reduction procedure using lysine as the capping and linker regents. The as-synthesized Au/ZnO hybrid nanorods possess the advantages of 1D nanostructure and the unique properties of Au nanoparticles. Gas sensing tests show that the Au/ZnO sensor manifests higher response (33.6–100 ppm ethanol at 380 °C), faster response and recovery time (3 s and 1 s) and better selectivity to ethanol in comparison to pure ZnO. The Au/ZnO sensor also has a wide detection range for ethanol concentration of 2–1000 ppm. The gas sensing mechanism of Au/ZnO hybrid nanorods is also discussed.

2. Experimental

2.1. Chemicals

Chemicals including zinc nitrate ($Zn(NO_3)_2{\cdot}6H_2O$), sodium dodecastyle benzene sulfonate ($C_{18}H_{29}NaO_3S$, SDBS), sodium hydroxide (NaOH), lysine, sodium borohydride ($NaBH_4$) as well as $HAuCl_4{\cdot}4H_2O$ used in the experiments were analytic grades without further treatment and purchased from Sinopharm, China. Distilled water (resistance higher than 18.2 MΩ cm) was used throughout the experiments.

2.2. Synthesis of ZnO nanorods

ZnO nanorods were synthesized *via* a modified hydrothermal process [28]. In a typical synthesis process, 1.19 g $Zn(NO_3)_2{\cdot}6H_2O$, 1.39 g SDBS and 4.0 g NaOH were dissolved into 40 mL ethanol under stirring. After 10 min, the solution was transferred into a 50 mL Teflon-lined autoclave, which was maintained at 100 °C for 10 h. Then the autoclave cooled down to room temperature naturally. The precipitates were washed several times with distilled water and ethanol alternatively, and dried at 60 °C overnight.

2.3. Synthesis of Au/ZnO hybrid

The synthesis of Au/ZnO hybrid nanorods followed the literature method [11]. Due to its abundant functional groups, lysine was utilized as both linker and capping agents to attach the Au nanoparticles onto the surface of ZnO nanorods. 0.3 g ZnO nanorods was dispersed in 40 mL water under stirring, at the same time, 1 mL (0.01 M) lysine was added into the aqueous solution. After stirring for 10 min, 0.2 mL (0.01 M) $HAuCl_4$ was introduced into the reaction system. Meanwhile, 5 mL (0.01 M) freshly prepared $NaBH_4$ was added into the mixture. After stirring for 30 min, the solution was centrifuged in order to obtain the samples. After drying at 60 °C, the purple powder was calcined at 300 °C for 30 min to remove lysine.

2.4. Characterizations

Phase identification was performed by power X-ray diffraction (XRD) using a Bruker diffractrometer (D8-Advance) with Cu Kα radiation of 1.5418 Å. The morphologies of the prepared ZnO as well as Au/ZnO nanorods were observed by scanning electron microscope (SEM, Quanta FEG 250, 30 kV) and transmission electron microscope (TEM, JEOL-1400, 100 kV), respectively. The elemental composition is tested by energy dispersive X-ray spectroscopy (EDS). The optical absorption property of Au/ZnO was characterized with UV-VIS-NIR spectrometer (UV-3600, Shimadzu).

2.5. Gas sensor fabrication and test

Details of gas sensor fabrication can be found in our former work [29]. A small amount of sample was ground in an agate mortar with several drops of distilled water to make the powder into a homogeneous paste. Then the paste was coated on an aluminum tube with length of 4 mm and diameter of 1 mm. Two Au electrodes and four Pt wires were positioned on both ends of the tube and a Ni–Cr alloy coil through the tube worked as a heater. For comparison, two gas sensors were fabricated using Au/ZnO and pure ZnO nanorods, respectively. Fig. 1(a) shows the optical photographs of the two sensors.

The devices performances were evaluated on a WS-60A gas sensing system at a relative humidity of 17% and the measuring principle is shown in Fig. 1(b). The sensors were placed into a transparent testing chamber whose volume is 20 L. Target gas was injected into the chamber by a microsyringe. During the gas sensing test, atmosphere air was used as the reference and diluting gas. The sensor response is defined as $S = R_a/R_g$, where R_a and R_g are the electrical resistance of the sensor in air and in target gas, respectively.

3. Results and discussion

3.1. Characterization

The phase and crystal structure of the samples have been identified by XRD. Fig. 2 shows the XRD patterns of the ZnO and Au/ZnO nanorods. The diffraction peaks in Fig. 2(a) can be well indexed to the wurtzite ZnO with hexagonal structure (JCPDS No. 80-0075). ZnO nanorods are well crystallized and no peaks for other impurities are found. Fig. 2(b) shows that the hybrid sample has a similar diffraction pattern to that of pure ZnO. By close observation three weak diffraction peaks can be seen at 38.2°, 44.4° and 64.6°, which can be attributed to metallic Au (JCPDS No. 89-3697). The weak diffraction peaks of Au indicate a small amount and a nanometer size in the hybrid materials.

The morphology and structure of the samples were investigated by SEM and TEM. In Fig. 3(a), ZnO nanorods show a 1D structure

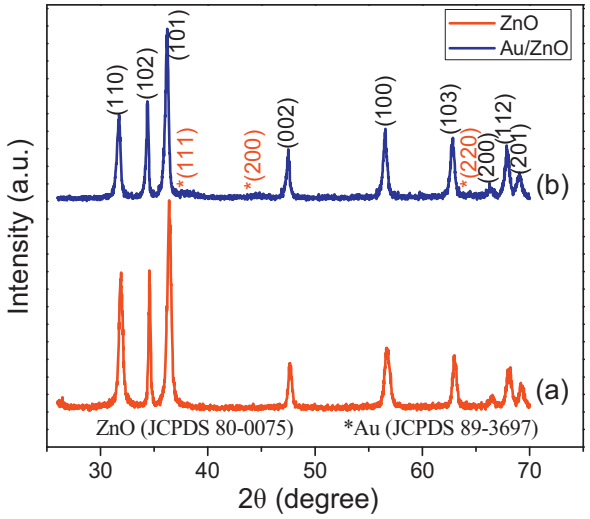

Fig. 2. XRD patterns of the ZnO (JCPDS 80-0075) and Au/ZnO nanorods. Weak peaks in (b) are from Au (JCPDS 89-3697) nanoparticles.

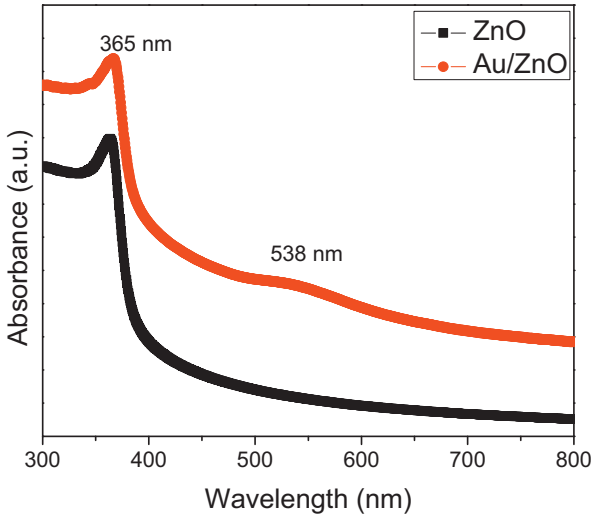

Fig. 4. UV–vis absorption spectra of ZnO and Au/ZnO nanorods.

with clean surface. The nanorods have a diameter of 30–50 nm and a length ranging from 200 to 600 nm. Fig. 3(b) displays the SEM image of Au/ZnO nanorods. In contrary to the smooth surface of ZnO nanorods, there are many Au nanoparticles coating on the ZnO nanorods, making the nanorod surface very rough. To prove the existence of Au nanoparticles on ZnO, we further use TEM to observe the hybrid nanorods. Fig. 3(c–e) shows the TEM images of Au/ZnO nanorods with different magnifications. A large amount of Au nanoparticles are seen to uniformly cover on the ZnO nanorods. From Fig. 3(e) the diameter of Au nanoparticles is estimated to be in the range of 3–6 nm. The content of Au in the hybrid materials has been tested by EDS. Fig. 3(f) is the EDS corresponding to sample in Fig. 3(b). It reveals that the nanorods are composed of Zn, O and Au, and the atomic percentage of Au in the hybrid sample is about 0.7%, corresponding to a mass content of 3.4%.

The presence of Au nanoparticles in the hybrids was further proved by UV–vis absorption spectrum. Fig. 4 is the absorbance spectra of ZnO and Au/ZnO nanorods. As can be seen from the plots, both the two curves show an absorption band at 365 nm which is known as the band edge absorption of ZnO. In addition, Au/ZnO shows another peak at 538 nm, which is due to the surface plasmon

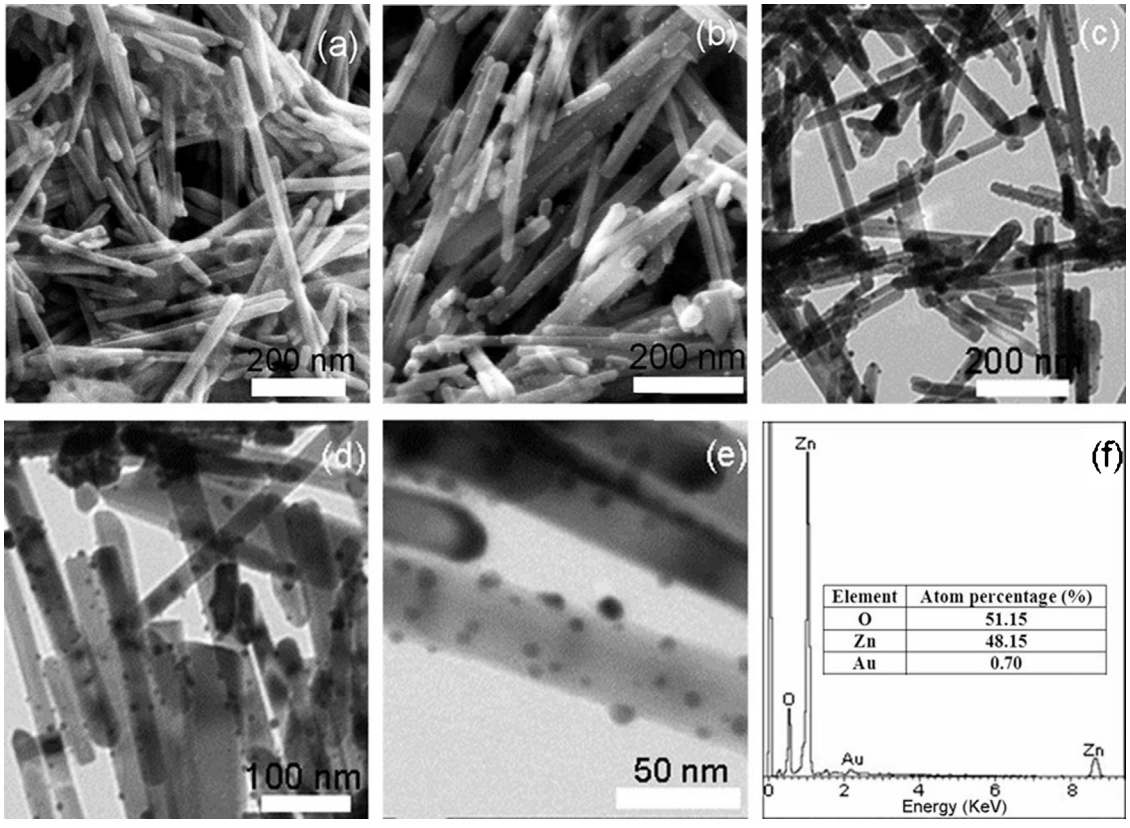

Fig. 3. SEM images of (a) ZnO nanorods and (b) Au/ZnO nanorods, (c–e) TEM of Au/ZnO nanorods, and (f) EDS analysis.

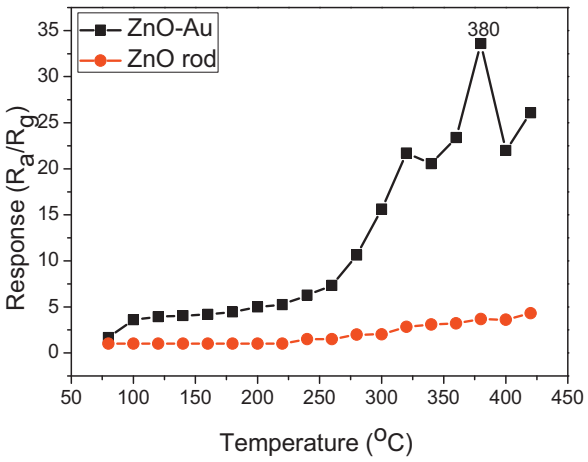

Fig. 5. Response of ZnO and Au/ZnO nanorods sensors to 100 ppm ethanol measured at the temperature range from 80 °C to 420 °C.

resonance of Au nanoparticles [30]. This further clearly indicated the successful loading of Au nanoparticles on the ZnO surface.

3.2. Gas sensing performance

Considering the hybrid Au/ZnO nanorods possess both the advantages of 1D nanostructure and catalytic Au nanoparticle, it is thus very interesting to apply the Au/ZnO nanorods to gas sensing. The working temperature plays an important role in the response of a gas sensor, because the temperature influences the reaction kinetics and the category and concentration of surface oxygen species [31]. Parallel tests to 100 ppm ethanol were carried out in the range of 80–420 °C in order to find out the optimum operating temperature of the sensors. In Fig. 5, the response of both sensors increases with the increasing working temperature. At a relative low temperature of 80 °C, the two sensors exhibit weak response to ethanol. Before 240 °C, the two curves are almost parallel, while after this temperature, the response of Au/ZnO increased significantly and reached a maximum value (33.6) at 380 °C, which is nearly 10 times higher than that (3.7) of ZnO. Moreover, the Au/ZnO has a much higher response than that of ZnO sensor at all temperatures, which is probably due to the sensitization of Au nanoparticles. Therefore we defined 380 °C as the optimum operating temperature of the Au/ZnO sensor and all the following tests of both sensors were performed at 380 °C.

Fig. 6(a) plots the response curves of sensors in real-time at 380 °C to different concentrations of ethanol. With the increase of ethanol concentration, the value of real-time response of both sensors increases apparently. The existence of Au makes the response amplitude changing extremely huge and far more in evidence. The response-recovery time is also an important parameter for application of sensors. Herein, we define these two parameters as the time required to reach 90% of the response change. Fig. 6(b) is the

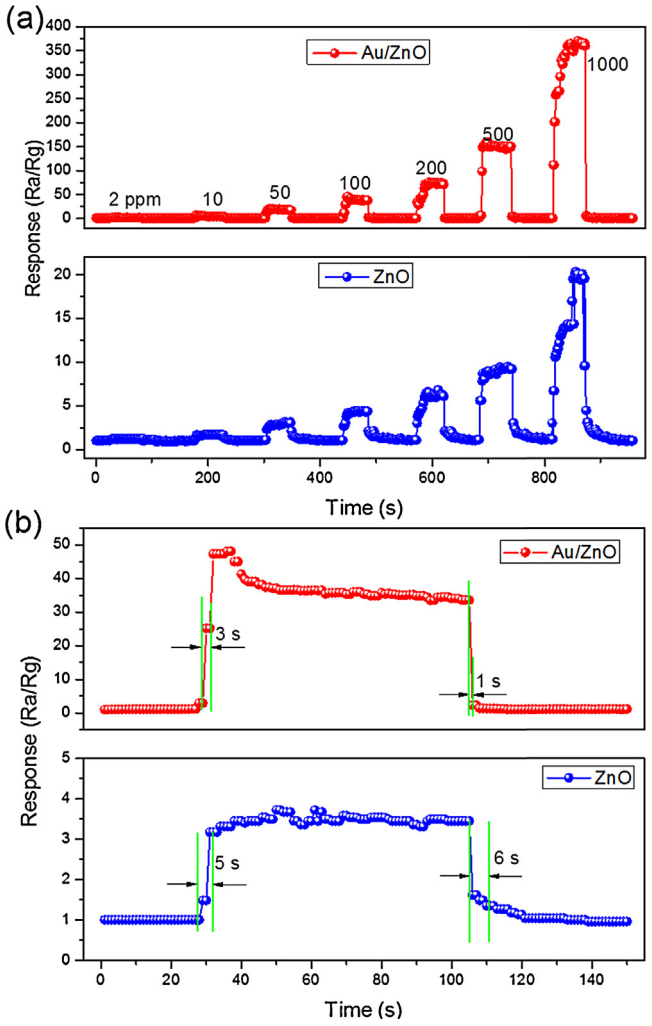

Fig. 6. (a) Sensor response curves to different concentrations of ethanol at 380 °C, and (b) corresponding response–recovery time to 100 ppm ethanol. Red and blue curves are for Au/ZnO and ZnO sensors, respectively. (For interpretation of the references to color in this figure legend, the reader is referred to the web version of this article.)

response curves of the two sensors to 100 ppm ethanol at 380 °C. The response time of ZnO nanorods is 5 s and the recovery time is 6 s. This performance is better than the results reported in literature [32,33]. Although the ZnO nanorods have fast response and recovery, the Au/ZnO sensor works even faster. Its response and recovery time are only 3 s and 1 s, respectively. Table 1 presents a comparison between the gas sensing performances of the Au/ZnO nanorods and former reported results. As shown in Table 1, although the operating temperature of the Au/ZnO sensor in this work is 380 °C, higher than or comparative to that of literature results, the Au/ZnO sensor

Table 1
Performance comparison of various ZnO-based gas sensors toward ethanol.

	Operating temperature (°C)	Ethanol (ppm)	Sensor response	Response time (s)	Recovery time (s)
Au-doped ZnO nanowires [25]	240	1000	37	–	–
ZnO spheres [32]	280	100	25	>10	>15
ZnO nanorods [33]	400	1000	360	17	6
ZnO nanotube [34]	300	100	24.1	3 (90%)	30 (98%)
Ti/ZnO nanotetrapods [35]	240	100	11.5	90	186
ZnO/Al thin film [36]	250	400	~20	~180	~180
Au/ZnO nanorods [23]	300	100	~5	–	–
ZnO microsphere [37]	420	5	~2.2	4	6
Au/ZnO in this paper	380	100	33.6	3	1

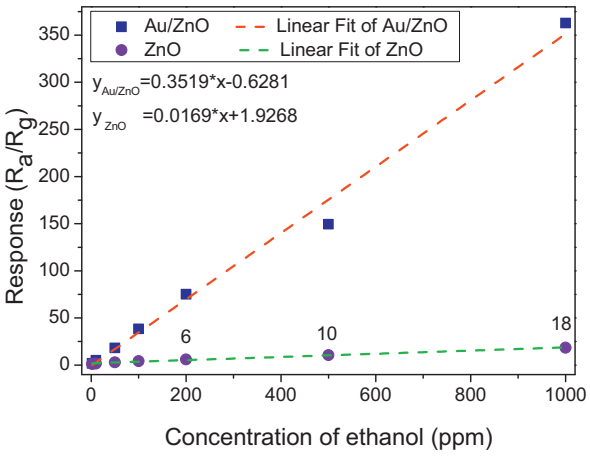

Fig. 7. The relation between the sensor sensitivity and ethanol concentration measured at 380 °C. Square dots and circle dots are experimental data for Au/ZnO and ZnO sensor, respectively, and the straight lines are the corresponding linear fit results.

demonstrates a much higher response to 100 ppm ethanol and very fast response-recovery speed.

Fig. 7 shows the sensor response as a function of ethanol concentration. It can be seen the Au/ZnO sensor has much higher responses than that of ZnO. To study the response dependence on the target gas concentration, the curves are linearly fitted as shown in Fig. 7. Obviously, the response increases in proportion to the gas concentration. The slope of Au/ZnO nanorod sensor is 0.3513, which is 20 times of ZnO sensor (0.0169). This implies that the Au/ZnO nanorod sensor is more sensitive than the ZnO sensor. When the ethanol concentration is changed, the alteration in sensor response of Au/ZnO is much larger than pristine ZnO. Furthermore, we can also find that the fitted response plot exhibits good linearity in a wide concentration from 2 to 1000 ppm, which is highly desirable for practical application.

Fig. 8(a) and (b) are the response curves of the Au/ZnO sensor for 7 cycles to 100 ppm ethanol at 380 °C before and after two months. Both the two curves exhibit good repeatability with fast response and recovery, although the response value after two months declines obviously. We suppose the decrease in response may be caused by the sintering of active materials after a long time working at 380 °C.

Beside ethanol, the Au/ZnO nanorod gas sensor was also tested for methanol and acetone sensing to evaluate the sensor selectivity. Fig. 9 compares the Au/ZnO sensor responses to various concentrations of different gases. Response value increases obviously to all the target gases with the increase of gas concentration. To ethanol, it has the largest response value to all the test concentrations, indicating the Au/ZnO sensor is more sensitive and selective to ethanol. The high response of Au/ZnO gas sensor manifested the potential application in ethanol detection.

3.3. Gas sensing mechanism

ZnO is a typical n-type semiconductor and its conductivity is influenced by the surface depletion layer, especially for nanostructures. Therefore, the mechanism of ZnO nanorod gas sensor is based on the change of resistance [3]. The target gas molecules adsorb onto or desorb from the working material surface, which can cause its resistivity change. That is the sensor response and recovery process. The nanorod shows high surface-to-volume ratio, high mobility of electrons along the axial direction which is beneficial for the sensing reactions occurring on the ZnO surface. When the sensor is placed in air, oxygen molecules will adsorb on the surface of

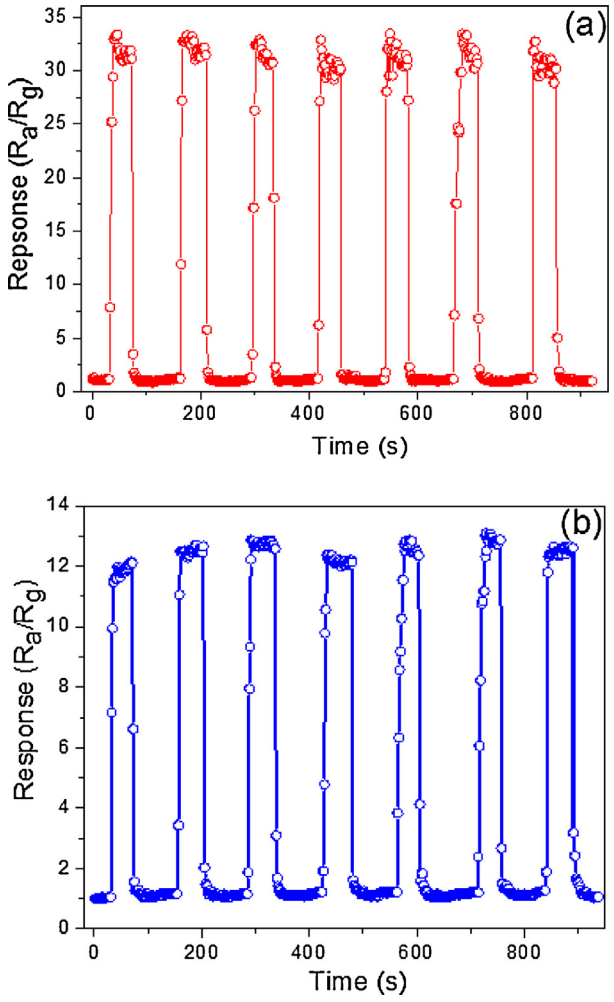

Fig. 8. The stability of Au/ZnO gas sensor, (a) response curve to 100 ppm ethanol of the as-prepared sensors measured at 380 °C and (b) similar data measured after two months.

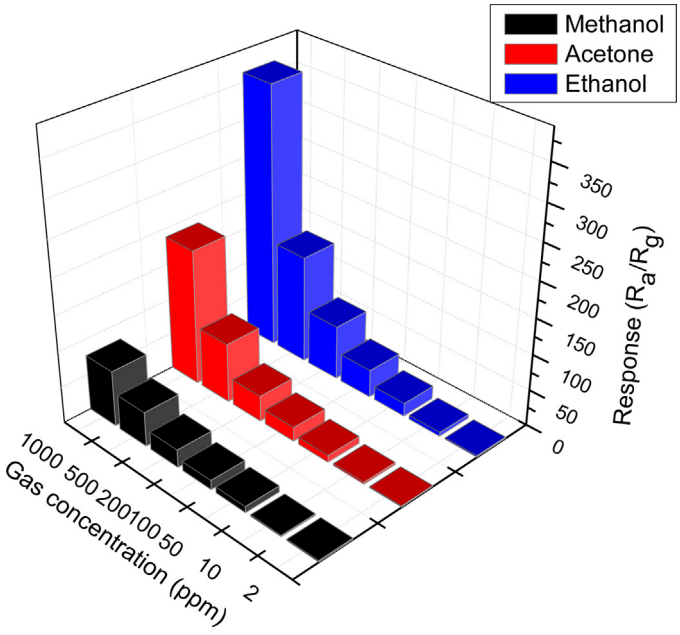

Fig. 9. Response histogram of Au/ZnO gas sensor to methanol, acetone and ethanol with different concentrations.

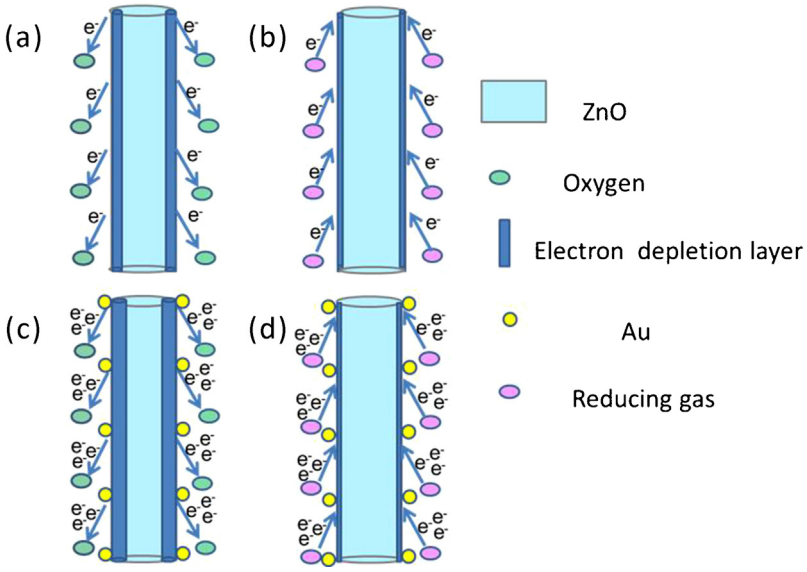

Fig. 10. Schematic gas sensing mechanism of ZnO and Au/ZnO nanorods. (a) Oxygen molecules were adsorbed and an electron depletion layer was formed on the surface of ZnO. (b) Oxygen species react with ethanol and release electrons back to the conduction band and thinner the electron depletion layer. (c) The existence of Au will lead to a thicker electron depletion layer compared with (a). (d) The electron depletion layer will be thinner compared with (b) and the response will be more obvious.

ZnO and capture electrons from the surface layer and change into oxygen species (O_2^-, O^- and O^{2-}). At the same time an electron depletion layer forms on the surface, as shown in Fig. 10(a). Here, the concentration of electrons, as majority carrier, is very low and the resistance is relatively large. When ethanol is injected into the test chamber, oxygen species (O_2^-, O^- and O^{2-}) would react with the reducing gas. The reaction can be depicted as follows [23]:

$$C_2H_5OH + 6O^- \rightarrow 2CO_2 + 3H_2O + 6e^-$$

Oxygen species react with ethanol and release electrons back to the conduction band of ZnO. The width of electron depletion layer decreases, leading to decrease in the sensor resistance, as shown in Fig. 10(b).

Compared with the ZnO gas sensor, the loading of Au nanoparticles onto ZnO nanorods improves their gas sensing performance. Firstly, Au nanoparticles on nanorods could increase the adsorption of oxygen molecules due to its spillover effect. This chemical mechanism of Au nanoparticles will make more electrons be trapped and the electron depletion layer will be thicker. It will generate more oxygen species and more reactive sites compared with the pristine ZnO, as shown in Fig. 10(a) and (c). When Au/ZnO was exposed to ethanol, more electrons will be fed back to the conduction band and decrease the width of electron depletion layer as illustrated in Fig. 10(b) and (d). Secondly, the electron mechanism could interpret the formation of depletion region around the noble nanoparticles which improve the modulation of nano-Schottky barriers during the oxidation of ethanol [38]. In addition, Au nanoparticles are also extensively used for catalysis. During the gas sensing test, Au might also plays the role of catalyst, which accelerates the kinetics of surface sensing reactions, leading to fast response–recovery.

4. Conclusions

In summary, a high performance gas sensor based on Au/functionalized ZnO nanorods was fabricated and demonstrated superior gas sensing performance in comparison to ZnO. The successful decoration of Au nanoparticles on ZnO nanorods plays a crucial role in improving the gas sensing properties. The Au/ZnO sensor manifests high response, fast response–recovery time and good repeatability, resulting from the combination of 1D nanostructure with unique properties of Au nanoparticles. The superior sensing features indicate the present Au/ZnO nanorods are promising for gas sensors.

Acknowledgments

This work is supported from MOE, China (NCET-11-1027, 213021A) and Shandong Provincial Science Foundation (JQ201214, BS2012CL003). BC thanks the Taishan Scholar Professorship (TSHW20091007) and JZ thanks the Research Fund (XKY11111) for new Faculty both tenured at University of Jinan.

References

[1] J. Zhang, J. Guo, H.Y. Xu, B.Q. Cao, Reactive-template fabrication of porous SnO_2 nanotubes and their remarkable gas-sensing performance, ACS Appl. Mater. Interfaces 5 (2013) 7893–7898.
[2] E. Comini, G. Faglia, G. Sberveglieri, Z.W. Pan, Z.L. Wang, Stable and highly sensitive gas sensors based on semiconducting oxide nanobelts, Appl. Phys. Lett. 81 (2002) 1869–1871.
[3] X.H. Liu, J. Zhang, L.W. Wang, T.L. Yang, X.Z. Guo, S.H. Wu, S.R. Wang, 3D hierarchically porous ZnO structures and their functionalization by Au nanoparticles for gas sensors, J. Mater. Chem. 21 (2011) 349–356.
[4] M. Law, L.E. Greene, J.C. Johnson, R. Saykally, P.D. Yang, Nanowire dye-sensitized solar cells, Nat. Mater. 4 (2005) 455–459.
[5] J.F. Ye, H.J. Zhang, R. Yang, X.G. Li, L.M. Qi, Morphology-controlled synthesis of SnO_2 nanotubes by using 1D Silica mesostructures as sacrificial templates and their applications in lithium-ion batteries, Small 6 (2010) 296–306.
[6] P.D. Yang, H.Q. Yan, S. Mao, R. Russo, J. Johnson, R. Saykally, N. Morris, J. Pham, R.R. He, H.J. Choi, Controlled growth of ZnO nanowires and their optical properties, Adv. Funct. Mater. 12 (2002) 323–331.
[7] A.B. Djurisic, Y.H. Leung, Optical properties of ZnO nanostructures, Small 2 (2006) 944–961.
[8] D.-J. Lee, H.-M. Kim, J.-Y. Kwon, H. Choi, S.-H. Kim, K.-B. Kim, Structural and electrical properties of atomic layer deposited Al-doped ZnO films, Adv. Funct. Mater. 21 (2011) 448–455.
[9] M.H. Huang, S. Mao, H. Feick, H.Q. Yan, Y.Y. Wu, H. Kind, E. Weber, R. Russo, P.D. Yang, Room-temperature ultraviolet nanowire nanolasers, Science 292 (2001) 1897–1899.
[10] J.S. Lee, O.S. Kwon, D.H. Shin, J. Jang, WO_3 nanonodule-decorated hybrid carbon nanofibers for NO_2 gas sensor application, J. Mater. Chem. A 1 (2013) 9099–9106.
[11] X.H. Liu, J. Zhang, X.Z. Guo, S.H. Wu, S.R. Wang, Amino acid-assisted one-pot assembly of Au, Pt nanoparticles onto one-dimensional ZnO microrods, Nanoscale 2 (2010) 1178–1184.

[12] I.-S. Hwang, S.-J. Kim, J.-K. Choi, J. Choi, H. Ji, G.-T. Kim, G. Cao, J.-H. Lee, Synthesis and gas sensing characteristics of highly crystalline ZnO–SnO_2 core–shell nanowires, Sens. Actuators B: Chem. 148 (2010) 595–600.
[13] G.G. Mandayo, E. Castano, F.J. Gracia, A. Cirera, A. Cornet, J.R. Morante, Strategies to enhance the carbon monoxide sensitivity of tin oxide thin films, Sens. Actuators B: Chem. 95 (2003) 90–96.
[14] N.S. Ramgir, M. Kaur, P.K. Sharma, N. Datta, S. Kailasaganapathi, S. Bhattacharya, A.K. Debnath, D.K. Aswal, K. Gupta, Ethanol sensing properties of pure and Au modified ZnO nanowires, Sens. Actuators B: Chem. 187 (2013) 313–318.
[15] Y.L. Cao, H.Y. Luo, D.Z. Jia, Low-heating solid-state synthesis and excellent gas-sensing properties of alpha-Fe_2O_3 nanoparticles, Sens. Actuators B: Chem. 176 (2013) 618–624.
[16] L.M. Huang, H.Q. Fan, Room-temperature solid state synthesis of ZnO/α-Fe_2O_3 hierarchical nanostructures and their enhanced gas-sensing properties, Sens. Actuators B: Chem. 171 (2012) 1257–1263.
[17] S.S. Ma, R. Li, C.P. Lv, W. Xu, X.L. Gou, Facile synthesis of ZnO nanorod arrays and hierarchical nanostructures for photocatalysis and gas sensor applications, J. Hazard. Mater. 192 (2011) 730–740.
[18] P. Sun, Z. Zhu, P.L. Zhao, X.S. Liang, Y.F. Sun, F.M. Liu, G.Y. Lu, Gas sensing with hollow α-Fe_2O_3 urchin-like spheres prepared via template-free hydrothermal synthesis, Cryst. Eng. Commun. 14 (2012) 8335–8337.
[19] J. Zhang, X.H. Liu, S.H. Wu, B.Q. Cao, S.H. Zheng, One-pot synthesis of Au-supported ZnO nanoplates with enhanced gas sensor performance, Sens. Actuators B: Chem. 169 (2012) 61–66.
[20] J. Zhang, X.H. Liu, L.W. Wang, T.L. Yang, X.Z. Guo, S.H. Wu, S.R. Wang, S.M. Zhang, Au-functionalized hematite hybrid nanospindles: general synthesis, gas sensing and catalytic properties, J. Phys. Chem. C 115 (2011) 5352–5357.
[21] L.L. Wang, H.M. Dou, Z. Lou, T. Zhang, Encapsuled nanoreactors (Au@SnO_2): a new sensing material for chemical sensors, Nanoscale 5 (2013) 2686–2691.
[22] C.C. Li, L.M. Li, Z.F. Du, H.C. Yu, Y.Y. Xiang, Y. Li, Y. Cai, T.H. Wang, Rapid and ultrahigh ethanol sensing based on Au-coated ZnO nanorods, Nanotechnology 19 (2008) 1–4.
[23] C.M. Chang, M.H. Hon, I.C. Leu, Influence of size and density of Au nanoparticles on ZnO nanorod arrays for sensing reducing gases, J. Electrochem. Soc. 160 (2013) B170–B176.
[24] L.W. Wang, S.R. Wang, M.J. Xu, X.J. Hu, H.X. Zhang, Y.S. Wang, W.P. Huang, A Au-functionalized ZnO nanowire gas sensor for detection of benzene and toluene, Phys. Chem. Chem. Phys. 15 (2013) 17179–17186.
[25] N. Hongsith, C. Viriyaworasakul, P. Mangkomtong, N. Mangkorntong, S. Choopun, Ethanol sensor based on ZnO and Au-doped ZnO nanowires, Ceram. Int. 34 (2008) 823–826.
[26] L.L. Wang, Z. Lou, T. Fei, T. Zhang, Templating synthesis of ZnO hollow nanospheres loaded with Au nanoparticles and their enhanced gas sensing properties, J. Mater. Chem. 22 (2012) 4767–4771.
[27] W. Wang, X.J. Wang, Y.L. Liu, Enhanced acetone sensing performance of Au nanoparticles functionalized flower-like ZnO, Rare Metal Mater. Eng. 42 (2013) 1699–1702.
[28] B. Liu, H.C. Zeng, Hydrothermal synthesis of ZnO nanorods in the diameter regime of 50 nm, J. Am. Chem. Soc. 125 (2003) 4430–4431.
[29] J. Guo, J. Zhang, D.X. Ju, H.Y. Xu, B.Q. Cao, Three-dimensional SnO_2 microstructures assembled by porous nanosheets and their superior performance for gas sensing, Powder Technol. 250 (2013) 40–45.
[30] T.A. El-Brolossy, T. Abdallah, M.B. Mohamed, S. Abdallah, K. Easawi, S. Negm, H. Talaat, Shape and size dependence of the surface plasmon resonance of gold nanoparticles studied by photoacoustic technique, Eur. Phys. J.: Special Top. 153 (2008) 361–364.
[31] Y. Cai, H.Q. Fan, M.M. Xu, Q. Li, C.B. Long, Fast economical synthesis of Fe-doped ZnO hierarchical nanostructures and their high gas-sensing performance, Cryst. Eng. Commun. 15 (2013) 7339–7345.
[32] W.C. Wang, Y.T. Tian, X.C. Wang, H. He, Y.R. Xu, C. He, X.J. Li, Ethanol sensing properties of porous ZnO spheres via hydrothermal route, J. Mater. Sci. 48 (2013) 3232–3238.
[33] L.X. Zhang, Y.Y. Yin, Large-scale synthesis of flower-like ZnO nanorods via a wet-chemical route and the defect-enhanced ethanol-sensing properties, Sens. Actuators B: Chem. 183 (2013) 110–116.
[34] Y.J. Chen, C.L. Zhu, G. Xiao, Ethanol sensing characteristics of ambient temperature sonochemically synthesized ZnO nanotubes, Sens. Actuators B: Chem. 129 (2008) 639–642.
[35] K.B. Zheng, L.L. Gu, D.L. Sun, X.L. Mo, G.R. Chen, The properties of ethanol gas sensor based on Ti doped ZnO nanotetrapods, Mater. Sci. Eng. B: Adv. Funct. Solid State Mater. 166 (2010) 104–107.
[36] S.M. Chou, L.G. Teoh, W.H. Lai, Y.H. Su, M.H. Hon, ZnO–Al thin film gas sensor for detection of ethanol vapor, Sensors 6 (2006) 1420–1427.
[37] J. Rao, A. Yu, C.L. Shao, X.F. Zhou, Construction of hollow and mesoporous ZnO microsphere: a facile synthesis and sensing property, ACS Appl. Mater. Interfaces 4 (2012) 5346–5352.
[38] A. Kolmakov, D.O. Klenov, Y. Lilach, S. Stemmer, M. Moskovits, Enhanced gas sensing by individual SnO_2 nanowires and nanobelts functionalized with Pd catalyst particles, Nano Lett. 5 (2005) 667–673.

Biographies

Jing Guo is a graduate student focusing on oxide gas sensors for master degree at University of Jinan. She was awarded a B.Sc. degree in materials science and engineering from the same university in 2012.

Jun Zhang obtained his PhD degree from the Department of Chemistry, Nankai University in 2011. His research is focused on the synthesis and applications of functional nanomaterials.

Min Zhu is now studying for her Master's Degree at University of Jinan with a research interest covering dye-sensitized solar cell.

Dianxing Ju is currently studying for the M.S. degree in the Department of material science and Engineering, University of Jinan, China. Now his research interests focus on the nanostructured materials for the gas sensor applications.

Hongyan Xu is an Associate Professor at School of Materials Science and Engineering, University of Jinan. Her main research interests are the synthesis and fabrication of semiconductor nanomaterials and conductive polymer composite chemical gas sensors.

Bingqiang Cao is a Taishan Scholar Professor for material physics with University of Jinan. His research group focuses on semiconducting oxide thin films, heterostructures, nanostructures, and related devices.